Fresh properties of self-consolidating concrete using SCM

Kiran. B, Dr. Nagaraja. P. S

Abstract— **This paper presents the key properties of freshly mixed self-consolidating concrete (SCC) using rice husk ash (RHA). Air-entrained SCC mixtures were produced based on the water/binder (W/B) ratios of 0.30–0.40. RHA was used substituting 0–30% of cement by weight. The fresh properties investigated were filling ability, passing ability, segregation resistance, air content, and unit weight. The effects of RHA and W/B ratio on these properties were observed. Test results revealed that the fresh properties were significantly influenced by the W/B ratio and RHA content of concrete. RHA also affected air entrainment and decreased the unit weight of concrete**

Index Terms— **Air content, Filling ability, Mixture proportions, Passing ability, Portland cement, Supplementary cementing material, Rice husk ash, Self-consolidating concrete, Segregation resistance, Unit weight, Water/binder ratio**

I. INTRODUCTION

The construction of concrete structures needs thorough placement and proper consolidation of fresh concrete to obtain good hardened properties and durability. However, the appropriate placement and consolidation were not always achievable with ordinary concretes, even though placed by skilled laborers. The lack of skilled laborers is also a great concern in construction industry. To resolve these problems, the concept of self-consolidating concrete (SCC) first emerged in 1986 [1]. However, the first prototype of SCC was developed in Japan in 1988 [2]. Later Japan tailored and optimized the technology of SCC, and used it commercially in large construction of buildings and infrastructure. The use of SCC in civil engineering structures has spread to other countries during the last two decades.

SCC is a highly flowable concrete that spreads through packed reinforcing bars, fills all corners of the formwork, and achieves the compacted condition under self-weight [3,4]. It differs from ordinary concrete with respect to its performance in fresh and hardened states that are mainly driven by exceptional material components and mixture proportions. SCC incorporates several special ingredients such as high-range water reducer (HRWR), supplementary cementing material (SCM), and viscosity-enhancing admixture (VEA) in addition to the basic materials used for ordinary concrete. The proportions of component materials in SCC are also significantly different from those of ordinary concrete [5–7].

Kiran. B, Assistant Professor, Department of Civil Engineering, Atria Institute of Technology, Bangalore, Karnataka, India 560024

Dr. Nagaraja. P. S, Professor, Department of Civil Engineering, U.V.C.E, Bangalore University, Bangalore, Karnataka, India 560056

SCC includes much higher quantity of binder, lower water content, greater fine aggregate content, and lesser amount of coarse aggregate than ordinary concrete. The water to binder (W/B) ratio of SCC is also much lower than that of ordinary concrete. While ordinary concrete has the W/B ratio mostly above 0.40, SCC needs a W/B ratio that typically ranges from 0.25 to 0.40 [8–10].

The use of HRWR is vital to produce SCC. In general, HRWR improves the filling ability and passing ability of SCC. However, excessive dosage of HRWR results in very high fluidity that might cause instability or segregation problem. The incorporation of a suitable SCM can improve segregation resistance or stability, while maintaining good filling ability and passing ability in fresh SCC. Several well-known SCMs such as silica fume, fly ash, and ground granulated blast-furnace slag have been used to produce SCC [11, 12]. Similarly, rice husk ash (RHA) can be used in SCC. RHA is produced by incinerating rice husk, which is a by-product of rice milling industry. Controlled incineration of rice husks between 500 and 800 °C produces non-crystalline or amorphous RHA [13, 14]. The particles of RHA occur in cellular structure with a very high specific surface area [15]. Due to very high specific surface area, RHA can act as a viscosity enhancer for fresh concrete [16]. The exceptionally high specific surface area of RHA increases the water-retaining capacity, and thus enhances the viscosity of concrete mixture. The increased viscosity is required to prevent segregation in SCC. However, the extremely high specific surface area of RHA may cause filling ability and passing ability problems in SCC that can be overcome using an efficient HRWR, such as polycarboxylate copolymer. Nevertheless, no comprehensive research has been carried out to investigate the effects of RHA on the key properties of freshly mixed SCC.

In the present study, various SCC mixtures were produced incorporating RHA as a supplementary cementing material at different W/B ratios. The freshly mixed SCC mixtures were tested to determine filling ability, passing ability, segregation resistance, unit weight, and air content. Test results revealed the effects of RHA and W/B ratio on these fresh properties of SCC.

II. RESEARCH SIGNIFICANCE

The filling ability, passing ability, and segregation resistance are three essential properties of SCC. These three properties must be carefully maintained to achieve self-consolidation capacity (self-compactability) of concrete. The unit weight and air content are also important depending on the type of application of SCC. For example, adequate air content is essential for good freeze–thaw durability when SCC is intended to be used in cold-region countries. In the present study, the performance of various SCC mixtures incorporating RHA was investigated with respect to the aforementioned fresh properties. Test results showed the effects of RHA on filling ability, passing ability, segregation resistance, unit weight and air content of fresh concrete, and suggested the optimum RHA content for SCC. The research findings will be of special interest to the construction industry regarding the use of SCC in different structural and non-structural applications. In addition, the research outcomes will be useful for the rice-producing countries like India for possible utilization of RHA in producing SCC.

III. Materials and Methods

3.1. Concrete constituent materials

Crushed granite stone, gravel, pit sand, normal portland cement (C), amorphous (non-crystalline) RHA, normal tap water (W), polycarboxylate-based high-range water reducer (HRWR), and synthetic air-entraining admixture (AEA) were used to produce various SCC mixtures. A blend of 50% crushed granite stone and 50% gravel by weight were used as the coarse aggregate (CA). Pit sand acted as the fine aggregate (FA). The nominal maximum size of coarse aggregate was 19 mm and that of fine aggregate was 4.75 mm. Normal portland cement and RHA acted as the binder (B), wherein RHA was used as a supplementary cementing material (SCM). The normal tap water was used as the mix water to prepare the concretes.

The amorphous RHA used in the present study was collected from Vellore, Tamil Nadu, India. It was supplied in the processed form. RHA is typically processed through thermal treatment. Amorphous RHA is obtained when rice husks are burnt at the temperature of 500–800 °C [7, 13]. To use as an excellent supplementary cementing material, the fineness of RHA must be greater than that of cement. The fineness of RHA can be improved through grinding. Ball or hammer mills are usually used to grind the RHA to a fine powder.

The concrete constituent materials were tested to examine their suitability and to obtain the major physical properties required for the mixture proportioning of concretes. The major physical properties of the concrete constituent materials are given in Table 1. In addition, the particle size distributions of cement and RHA are shown in Fig. 1. Fine and coarse aggregates confirmed to the ASTM grading requirements [17]. RHA was much finer than cement. The median particle size of RHA was 6 µm and that of cement was 15 µm. The aggregate blends with different proportions of air-dry fine aggregate (pit sand) and air-dry coarse aggregate (crushed granite stone and gravel) were prepared and tested for bulk density, as shown in Fig. 2. The optimum sand to total aggregate (S/A) ratio of 0.50 leading to the maximum bulk density in aggregate blend was obtained from this figure.

Table 1

Major physical properties of concrete constituent materials.

Constituent material	Property
Coarse aggregate (CA)	Oven-dry based bulk density: 1670 kg/m³ Void content: 37% Saturated surface-dry based specific gravity: 2.71 Absorption: 1.5% Total evaporable moisture content: 0.1%
Fine aggregate (FA)	Oven-dry based bulk density: 1860 kg/m³ Void content: 28% Fineness modulus: 2.74 Saturated surface-dry based specific gravity: 2.62 Absorption: 1.0% Total evaporable moisture content: 0.1%
Normal portland cement (C)	Specific gravity: 3.16 Blaine specific surface area: 410 m²/kg % passing 45-lm (No. 325) wet sieve: 92%
Rice husk ash (RHA)	Specific gravity: 2.1 Blaine specific surface area: 2330 m²/kg
Normal tap water (W)	Solid content: 0.043% Density: 997.3 kg/m³
High-range water reducer (HRWR)	Specific gravity: 1.07 Solid content: 41%
Air-entraining admixture (AEA)	Specific gravity: 1.01 Solid content: 13%

Constituent material	Property
Coarse aggregate (CA)	Oven-dry based bulk density: 1670 kg/m³ Void content: 37% Saturated surface-dry based specific gravity: 2.71 Absorption: 1.5% Total evaporable moisture content: 0.1%
Fine aggregate (FA)	Oven-dry based bulk density: 1860 kg/m³ Void content: 28% Fineness modulus: 2.74 Saturated surface-dry based specific gravity: 2.62 Absorption: 1.0% Total evaporable moisture content: 0.1%
Normal Portland cements (C)	Specific gravity: 3.16 Blaine specific surface area: 410 m²/kg % passing 45-lm (No. 325) wet sieve: 92%
Rice husk ash (RHA)	Specific gravity: 2.1 Blaine specific surface area: 2330 m²/kg
Normal tap water (W)	Solid content: 0.043% Density: 997.3 kg/m³
High-range water reducer (HRWR)	Specific gravity: 1.07 Solid content: 41%
Air-entraining admixture (AEA)	Specific gravity: 1.01 Solid content: 13%

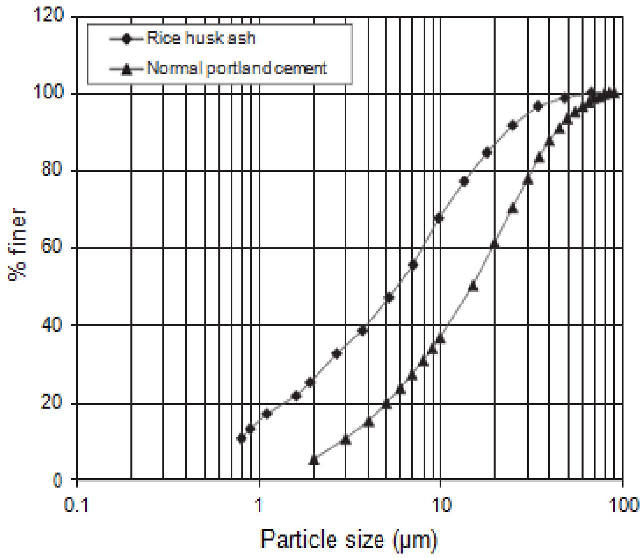

Fig. 1. Particle size distribution of normal portland cement and rice husk ash

3.2. Concrete mixture proportions

Different types of air-entrained SCC mixtures were designed based on the W/B ratios of 0.30, 0.35 and 0.40, and using RHA as 0–30% replacement of cement by weight. In addition, the optimum S/A ratio of 0.50 resulting in the maximum bulk density of aggregate blend was used to design the SCC mixtures. The design air content (total air content) was 6% for all air-entrained concrete mixtures. The quantity of mix water for the SCC mixtures was estimated and adjusted based on the ACI guideline given in ACI 211.4R-93 [18]. A minimum slump of 75–100 mm specified without any HRWR was considered for the first estimate of mix water requirement. However, the HRWR was used in all concretes to obtain the required level of filling ability and passing ability. The dosages of HRWR were varied for different concrete mixtures to achieve a slump ≥250 mm and a slump flow ≥600 mm. The AEA was incorporated with adequate dosages to obtain the concrete air content of 6 ± 1.5%. The details of concrete mixture proportions including HRWR and AEA dosages are given in Table 2.

3.3. Preparation of fresh concretes

The fresh SCC mixtures were prepared by a revolving pan type concrete mixer. The batch volume of the concrete mixtures was taken at least 15% more than the required to compensate the loss during mixing, sampling, and testing. The quantities of constituent materials for each concrete batch were determined based on the mixture proportions shown in Table 2. As the air-dry

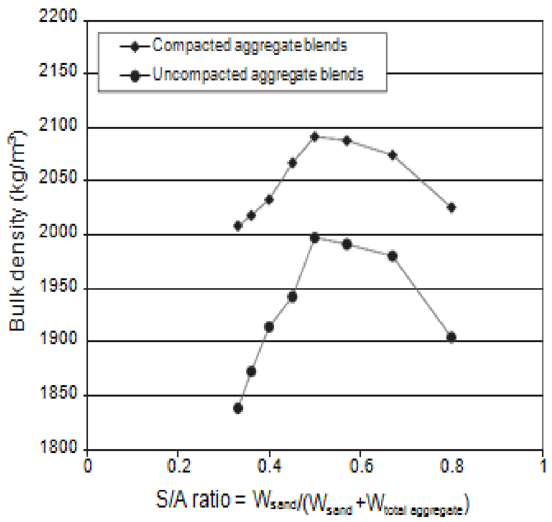

Fig. 2. Bulk density of different aggregate blends

aggregates were used, the proportions of fine and coarse aggregates obtained from Table 2 were corrected considering the absorption and moisture content of aggregates. Also, the amount of mix water was adjusted based on the absorption of aggregates and the water contribution of HRWR.

The coarse and fine aggregates were charged first into the mixer and mixed with one-quarter of the mix water for 1 min. Then the dosage of AEA dispensed in the second-quarter of the mix water was added and the mixing was continued for 1 min. The mixer was stopped thereafter and the binder (cement alone or with RHA) was charged into the mixer. Immediately, the mixer was restarted and the mixing was continued for 2 min with the addition of third-quarter of the mix water. After that, the mixer was stopped, and the concrete materials in the pan were covered with a piece of wet burlap and allowed to rest for 3 min. The rest period was intended to allow the air-dry aggregates to absorb some of the mix water, thus minimizing the likelihood for absorption of HRWR by the aggregates. At the end of rest period, the mixer was restarted and the mixing was continued for 3 min with the addition of HRWR dispensed in fourth-quarter of the mix water.

3.4. Testing of fresh concretes

3.4.1. Slump and slump flow test

The slump and slump flow of concrete were determined using an Abram's slump cone [19]. The slump cone was filled with fresh concrete in one layer and without any means of consolidation. Then the slump cone was lifted vertically in 3–5 s to allow the concrete sample to spread on the surface of a steel pan or sheet. The vertical drop of the concrete sample from its original position was measured and reported as the slump. The slump flow was measured from the same test conducted for determining the slump. The diameter of the deformed concrete was measured at two pairs of perpendicular (right-angle) positions that divided the flow patty into eight equal segments. The average diameter was recorded as the slump flow of concrete.

3.4.2. Slump cone–J-ring flow test

The slump cone–J-ring flow test was conducted to determine the J-ring slump and slump cone–J-ring flow spread of concrete. An Abram's slump cone [19] and a J-ring were used in this test. The J-ring was built using 10-mm deformed reinforcing bars. The spacing of the bars was 57 mm (three times the maximum size of coarse aggregate), which is greater than the minimum recommended bar spacing. The minimum recommended bar spacing for J-ring is 2.5 times the maximum size of coarse aggregate [20]. The details of the J-ring are shown in Fig. 3. The slump cone was placed at the center of the J-ring and filled with concrete in one layer without any consolidation. Then the slump cone was raised vertically in 3–5 s and the concrete was allowed to deform. The vertical drop of the concrete sample was measured in the presence of J-ring and reported as the J-ring slump. In addition, the diameter of the concrete spread through the J-ring was measured in a similar way as mentioned in the case of slump flow.

The average diameter was recorded as the slump cone–J-ring flow spread.

3.4.3. Orimet flow test

The orimet flow was determined using an orimet, as shown in Fig. 4. It had a 600 mm long Ø120 mm vertical pipe, which was welded with a 60 mm high conical orifice at the bottom end. The outlet diameter of the orifice can be varied. The orimet used in this study had an orifice with the outlet diameter of 80 mm. The orifice outlet level was at a height of 430 mm from the floor. A trap door was attached to the orifice. During testing, the fresh concrete was poured into the orimet pipe in one layer and without any means of consolidation, while keeping the trap door closed. Later the trap door was opened to allow the concrete to flow through the orifice. At the same time, a stopwatch was started to record the orimet flow time. In addition, the diameter of the deformed concrete was measured at four right-angle positions that divided the flow patty into eight equal segments. The average diameter was recorded as the orimet flow spread.

3.4.4 Orimet–J-ring flow test

The orimet–J-ring flow test was conducted to determine the orimet flow spread in the presence of a J-ring. A J-ring (refer to Section 3.4.2) and an orimet (refer to Section 3.4.3) were used in this test. The orimet was placed over the J-ring and the orifice of the orimet was centralized with the J-ring. The concrete was placed in the cast pipe of the orimet in one layer and without any consolidation. The trap door was opened, and the concrete was allowed to fall and deform through the J- ring. The diameter of the concrete spread through the J-ring was measured in a similar way as mentioned in the case of orimet flow spread. The average diameter was recorded as the orimet–J-ring flow spread.

3.4.5 Inverted slump cone flow test

The inverted slump cone flow was determined by using an Abram's slump cone [19] in its inverted position. The details of the inverted slump cone apparatus are shown in Fig. 5. The inverted slump cone was fixed through a circular hole made at the center of a rigid wooden table. A trap door was fastened at the bottom of the inverted slump cone. The constricted end of the inverted slump cone was at a height of 430 mm from the floor. The conical shape (the diameter is reduced from 200 to 100 mm over a depth of 300 mm) produced some resistance to the concrete flow. The fresh concrete was poured into the inverted slump cone in one layer and without any form of consolidation, while keeping the trap door closed. Then the trap door was opened to allow the concrete to flow out of the cone. Simultaneously, a stopwatch was used to record the inverted slump cone flow time of concrete. Moreover, the diameter of the deformed concrete was measured at four right-angle positions that divided the flow patty into eight equal segments. The average diameter was registered as the inverted slump cone flow spread.

3.4.6 Inverted slump cone–J-ring flow test

The inverted slump cone–J-ring flow test was conducted to determine the inverted slump cone flow spread in the presence of a J-ring. The test was carried out by using the inverted slump cone apparatus (refer to Section 3.4.5) along with a J-ring (refer to Section 3.4.2). The inverted slump cone apparatus was placed above the J-ring and the lower opening of the cone was vertically centralized with

Table 2

Details of SCC mixture proportions.

Concrete type	W/B ratio	CA (kg/m^3)	FA (kg/m^3)	C (kg/m^3)	RHA (kg/m^3)	W (kg/m^3)	HRWR (% B[a])	AEA (% B)
C30RHA0	0.30	846.3	842.2	492.7	0 (0% B)	147.8	0.875	0.026
C30RHA15	0.30	829.9	825.8	418.8	73.9 (15% B)	147.8	1.75	0.047
C30RHA20	0.30	824.4	820.3	394.2	98.5 (20% B)	147.8	2.10	0.056
C35RHA0	0.35	876.1	871.8	422.3	0 (0% B)	147.8	0.70	0.020
C35RHA5	0.35	871.4	867.1	401.2	21.1 (5% B)	147.8	0.875	0.025
C35RHA10	0.35	866.7	862.4	380.1	42.2 (10% B)	147.8	1.05	0.035
C35RHA15	0.35	862.0	857.8	359.0	63.3 (15% B)	147.8	1.40	0.045
C35RHA20	0.35	857.3	853.1	337.8	84.5 (20% B)	147.8	1.75	0.054
C35RHA25	0.35	852.6	848.4	316.7	105.6 (25% B)	147.8	2.10	0.070
C35RHA30	0.35	847.9	843.7	295.6	126.7 (30% B)	147.8	2.45	0.080
C40RHA0	0.40	898.4	894.0	369.5	0 (0% B)	147.8	0.60	0.011
C40RHA15	0.40	886.0	881.7	314.1	55.4 (15% B)	147.8	1.00	0.040
C40RHA20	0.40	881.9	877.6	295.6	73.9 (20% B)	147.8	1.20	0.051

[a] Binder = C + RHA

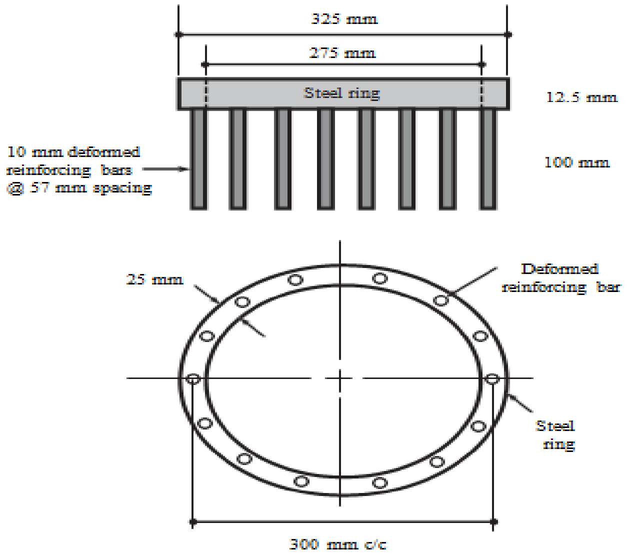

Fig. 3. Details of the J-ring

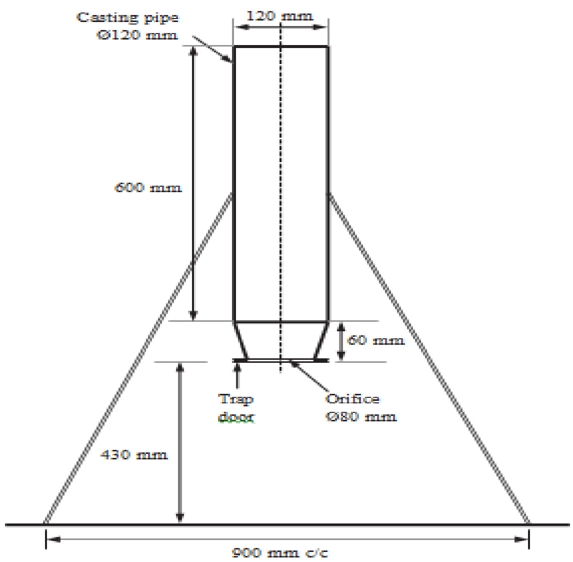

Fig. 4. Details of the orimet apparatus

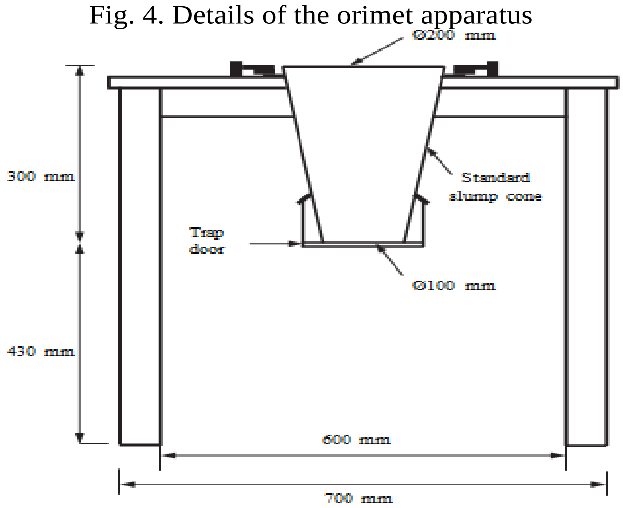

Fig. 5. Details of the inverted slump cone apparatus

the J-ring. The trap door was closed and the concrete was placed in the inverted slump cone in one layer and without any consolidation. Then the trapped door was opened, and the concrete was allowed to fall and flow through the J-ring. The diameter of the deformed concrete was measured in the presence of J-ring. The measurement was taken in a similar way as mentioned in the case of inverted slump cone flow spread. The average diameter was reported as the inverted slump cone–J-ring flow spread.

3.4.7 Visual inspection for segregation resistance The SCC mixtures were visually inspected after slump flow, orimet flow spread, and inverted slump cone flow spread tests to assess the segregation resistance of concrete based on the procedure used by Daczko [21]. The segregation resistance concrete was judged by observing the appearance of concrete with respect to aggregate pile, mortar halo, paste ring, and bleeding. The segregation resistance was rated with regard to visual stability index (VSI) varying in the range of 0–3. The non-segregating (highly stable) concrete with no sign of segregation was assigned a VSI value of ''0'' whereas the severely segregating (highly unstable) concrete was given a VSI value of ''3''.

3.4.8 Test for unit weight

The unit weight of various fresh SCC mixtures was determined using the measuring bowl of the air meter. The measuring bowl was calibrated prior to testing to determine its volume. The procedure stated in ASTM C 138/C 138M [22] was followed with some exceptions for filling and consolidation of concrete. Specifically, the measuring bowl was filled in one layer instead of three, and no means of consolidation was used during concrete filling. The weight of the concrete contained in the measuring bowl was determined. Later, the unit weight was computed from the known weight and volume of concrete.

3.4.9 Test for air content

The air content of the fresh SCC mixtures was determined by a Type B air meter [23]. The pressure method as depicted in ASTM C 231 [23] was used with some exceptions for pouring and consolidation of concrete. Specifically, the measuring bowl of the air meter was filled with the fresh concrete in one layer and without any means of consolidation. The air content obtained from the air meter was corrected for the aggregate content of the concrete to obtain the actual air content.

IV. TEST RESULTS AND DISCUSSION

4.1 Filling ability of concretes

The filling ability results of various SCC mixtures were obtained with respect to slump and slump flow, inverted slump cone flow (flow time and flow spread), and orimet flow

(flow time and flow spread). The liquefying and dispersing actions and the resulting water reduction capacity of HRWR [24–26] contributed to improve the filling ability ofconcrete. The adequate dosage of HRWR improved the deformability of concrete and thus resulted in high slump and slump flow, and good orimet flow and inverted slump cone flow spreads. In addition, the adequate dosage of HRWR made the concretes less viscous, and therefore no interrupted concrete flow or blocking of concrete flow leading to extremely high flow time occurred during orimet and inverted slump cone flow tests.

Table 3

Filling ability of different SCC mixtures.

Concrete type I	Slump (mm)	Slump-flow (mm)	Inverted slump cone flow		Orimet Flow	
			Flow time (s)	Flow spread (mm)	Flow time (s)	Flow spread (mm)
C30RHA0	275	710	3.8	680	6.6	750
C30RHA15	280	735	5.1	715	9.2	770
C30RHA20	275	770	6.2	725	11.5	780
C35RHA0	270	690	2.9	655	5.7	720
C35RHA5	270	700	3.2	660	6.4	730
C35RHA10	270	710	3.6	675	7.2	740
C35RHA15	280	720	3.9	690	7.6	760
C35RHA20	275	710	5.1	680	8.8	750
C35RHA25	275	740	5.4	700	9.6	775
C35RHA30	275	750	5.8	710	10.4	795
C40RHA0	265	665	2.3	615	4.8	690
C40RHA15	270	680	2.6	650	6.8	715
C40RHA20	265	675	2.8	660	7.1	720

4.1.1. Slump

The slump varied in the range of 265–280 mm (Table 3), which is consistent with the slump values reported in literature [27]. However, the measured slump values did not exhibit any significant relative differences among the filling ability of the concretes, since the variation of the slump was marginal. For example, the slump of C35RHA0 and C35RHA30 SCC mixtures was 270 and 275 mm, respectively. The slump increased by only 5 mm although the deformability of the concrete was significantly improved in the presence of 30% RHA. It suggests that the slump is not a suitable criterion to assess the filling ability of SCC.

4.1.2. Slump flow

The slump flow of the SCC mixtures varied from 665 mm to 770 mm (Table 3). This range of slump flow indicates an excellent filling ability of SCC; usually, the slump flow of SCC varies in the range of 600–850 mm [28–30]. Unlike the slump, there was significant variation in the slump flow results, thus exhibiting the relative differences in the filling ability of the concretes. For example, the slump flow of C35RHA0 and C35RHA30 SCC mixtures was 690 and 750 mm, respectively. The slump flow was significantly increased by 60 mm in the presence of 30% RHA. Hence, the slump flow is recommended instead of slump to assess the filling ability of SCC.

4.1.3. Orimet flow time

The orimet flow time of the SCC mixtures varied from 4.8 s to 11.5 s (Table 3). The maximum acceptable limit for the orimet flow time is 9 s [31]. The orimet flow time of the concretes C30RHA15, C30RHA20, C35RHA25, and C35RHA30 was slightly above this maximum limit. It suggests that these concretes were more viscous than the other concretes.

4.1.4. Orimet flow spread

The orimet flow spread of the concretes varied in the range of 690–800 mm following a similar trend as noticed in the case of slump flow (Table 3). However, it was greater than the slump flow by 10–45 mm. This result suggests that more kinetic energy was involved in the orimet flow spread of concrete. The increased kinetic energy was obtained due to a greater mass of concrete and also as a result of the higher falling height of concrete used in orimet test. The concrete sample used in orimet test was about 37% greater than that used in slump flow test. Furthermore, the concrete sample used in orimet test dropped from a height of 430 mm, which is higher than the overall sample height of 300 mm used in slump flow test.

4.1.5. Inverted slump cone flow time

The inverted slump cone flow time of the SCC mixtures varied from 2.3 s to 6.2 s following a similar trend as observed in the case of orimet flow time (Table 3). However, the inverted slump cone flow time was 42–62% lower than the orimet flow time of concrete. This is mostly due to the smaller mass of concrete used in inverted slump cone test. In addition, the outlet diameter of inverted slump cone was greater than that of orimet. The greater outlet diameter accelerated the flow of concrete.

4.1.6. Inverted slump cone flow spread

The inverted slump cone flow spread of the SCC mixtures varied in the range of 615–725 mm following a similar trend as observed in the cases of slump flow and orimet flow spread (Table 3). Also, the inverted slump cone flow spread was lower than the slump flow by 15–50 mm. It suggests that a lower kinetic energy was involved in the inverted slump cone flow spread, even though the mass of concrete was the same and the falling height of concrete sample was greater than the overall sample height used in slump flow test. The resistance caused by the constricted end of the inverted slump cone and the impact of concrete sample on the pan produced some loss of kinetic energy, thus decreasing the flow spread of concrete.

4.2. Passing ability of concretes

The passing ability results of the SCC mixtures were obtained with respect to J-ring slump, slump cone–J-ring flow spread, orimet– J-ring flow spread, and inverted slump cone–J-ring flow spread. The HRWR influenced the passing ability of concretes by influencing their filling ability. The adequate dosage of HRWR improved the filling ability, and thus maintained a good passing ability for the concretes. Therefore, a significant amount of concrete passed though the J-ring in all cases without any blocking.

4.2.1. J-ring slump

The J-ring slump varied in the range of 255–270mm for various SCC mixtures (Table 4). Similar to the slump, the J-ring slump varied in a narrow range indicating its unsuitability for measuring the passing ability of SCC.

4.2.2. Slump cone–J-ring flow spread

Unlike the J-ring slump, the slump cone–J-ring flow spread (Slump flow in the presence of J-ring) varied in the wide range of 650–740 mm (Table 4). The variation in slump cone–J-ring flow spread followed a similar trend as observed in the case of slump flow. However, the slump cone–J-ring flow spread was lower than the slump flow by 15–30 mm. The reduction in slump flow in the presence of a J-ring should not be greater than 50 mm to maintain a good passing ability [20]. Thus, the slump cone–J-ring flow spread results obtained in the present study exhibited good passing ability of the concretes.

Table 4

Passing ability of different SCC mixtures

Concrete type	J-ring slump (mm)	Slump-cone-J-ring flow spread (mm)	Inverted slump cone-J-ring flow spread (mm)	Orimet-J-ring flow spread (mm)
C30RHA0	265	680	660	730
C30RHA15	270	715	700	745
C30RHA20	265	740	710	765
C35RHA0	260	670	640	690
C35RHA5	260	680	645	695
C35RHA10	260	690	655	705
C35RHA15	270	700	665	720
C35RHA20	265	695	660	715
C35RHA25	265	715	670	760
C35RHA30	265	725	675	770
C40RHA0	255	650	595	675
C40RHA15	260	660	630	700
C40RHA20	255	655	645	705

Table 5

Visual rating of segregation resistance for different SCC mixtures

Concrete mixture	Criteria for visual inspection	Rating of segregation resistance	
		Stability	VSI[a] value
C30RHA0, C35RHA0, C40RHA0, C35RHA5	No bleeding, paste ring, mortar halo and aggregate pile in slump flow, and orimet flow and inverted slump cone flow spreads	Highly stable	0
C35RHA10, C40RHA15, C40RHA20	No bleeding and aggregate pile but negligible paste ring or mortar halo in slump flow, and orimet and inverted slump cone flow spreads	Stable	1
C30RHA15, C35RHA15, C35RHA20	No bleeding and aggregate pile but considerable paste ring or mortar halo in slump flow, and orimet and inverted slump cone flow spreads	Unstable	2
C30RHA20, C35RHA25, C35RHA30	No bleeding and aggregate pile but severe paste ring or mortar halo in slump flow, and orimet and inverted slump cone flow spreads	Highly unstable	3

[a] Visual stability index

4.2.3 *Orimet–J-ring flow spread*

The orimet–J-ring flow spread (orimet flow spread in the presence of J-ring) varied in the wide range of 675–770 mm (Table 4). The variation in orimet–J-ring flow spread followed a trend similar to that observed in orimet flow spread. However, the presence of J- ring decreased the orimet flow spread by 15–40 mm.

4.2.4 *Inverted slump cone–J-ring flowspread*

The inverted slump cone–J-ring flow of various SCC mixtures ranged from 595 to 710 mm (Table 4). The variation in the inverted slump cone–J-ring flow spread was similar to that of inverted slump cone flow spread. But the flow spread of the concretes was reduced in the presence of J-ring. The inverted slump cone– J-ring flow spread was lower than the inverted slump cone flow spread by 15–35 mm.

4.3 *Segregation resistance of concretes*

The results of visual inspection for the segregation resistance of different SCC mixtures are given in Table 5. No sign of segregation appeared in the slump flow, and orimet and inverted slump cone flow spreads of C30RHA0, C35RHA0, C35RHA5, and C40RHA0. Thus these four concretes were highly stable and rated with a VSI value of ‘‘0’’. Negligible mortar halo appeared in the flow spreads of C35RHA10, C40RHA15, and C40RHA20, and thus indicated their adequate segregation resistance. These three concretes were stable and rated with a VSI value of ‘‘1’’. Considerable mortar halo occurred in the flow spreads of C30RHA15, C35RHA15 and C35RHA20, and thus indicated their low segregation resistance. These concrete were unstable and rated with a VSI value of ‘‘2’’. Severe mortar halo emerged in the flow spreads of C30RHA20, C35RHA25 and C35RHA30, and thus indicated their poor segregation resistance. These three concretes were highly unstable and rated with a VSI value of ‘‘3’’. The physical appearances of the flow spreads of several concretes are shown in Figs. 6–8.

No sign of segregation for the concrete C35RHA0 (VSI = 0)

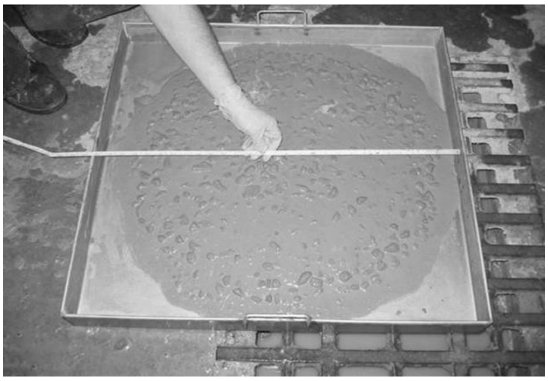

Severe mortar halo in C35RHA25 (VSI = 3)

Fig. 6. Visual appearance of concrete during slump and slump flow test.

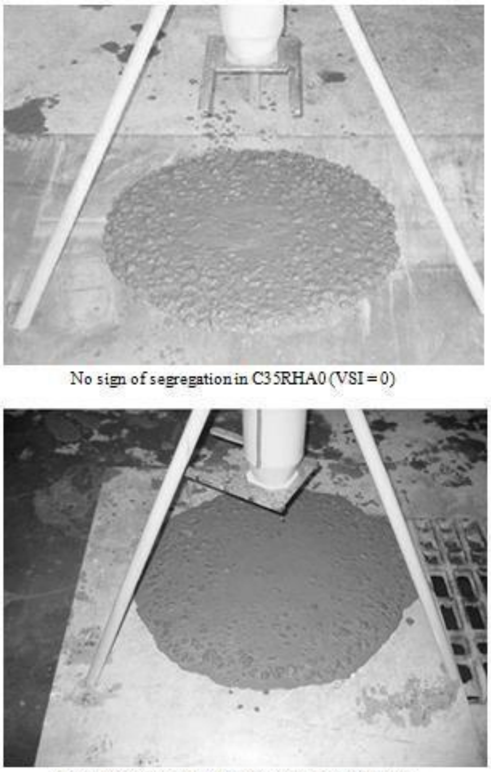

No sign of segregation in C35RHA0 (VSI = 0)

Considerable mortar halo in C35RHA15 (VSI = 2)

Fig. 7. Visual appearance of concrete during orimet flow test.

4.4 Unit weight of concretes

The results of unit weight for different SCC mixtures are presented in Table 6. The unit weight of the concretes varied in the range of 2255–2325 kg/m^3. Based on the measured air content of concrete and the batch weight of constituent materials, the unit weights for various SCC mixtures were also estimated. The estimated unit weight was lower than the measured unit weight by only 0.7–1.5%.

4.5 Air content of concretes

The results of air content for various SCC mixtures are shown in Table 6. The measured air contents were within ±1.0% of the design air content, which is acceptable. The maximum acceptable tolerance for air content measurement can be in the range of ±1.5% [29].

4.6 Effects of W/B ratio and RHA content on fresh concrete properties

4.6.1 Filling ability

The slump flow, orimet flow spread, and inverted slump cone flow spread increased significantly with lower W/B ratio and higher RHA content (Table 3). This is credited to the decreased aggregate content and increased paste volume of concrete. The paste volume of the concretes was increased with lower W/B ratio and higher RHA content (Table 7). In addition, the aggregate content was decreased at lower W/B ratio and higher RHA content (Tables 2 and 7). The slump flow increases with decreased aggregate con- tent and increased paste volume of the concrete [25, 33]. A similar

No sign of segregation in C35RHA0 (VSI = 0)

Considerable mortar halo in C35RHA15 (VSI = 2)

Fig. 8. Visual appearance of concrete during inverted slump cone flow test

Table 6

Unit weight and air content of different SCC mixtures

Concrete	Air Content (%)		Unit weight (kg/m^3)	
	Design	Measured	Estimated	Measured
C30RHA0	6	5.7	2290	2325
C30RHA15	6	5.3	2265	2280
C30RHA20	6	5.7	2245	2260
C35RHA0	6	5.3	2285	2315
C35RHA5	6	5.5	2275	2310
C35RHA10	6	5.1	2275	2310
C35RHA15	6	5.1	2265	2290
C35RHA20	6	5.0	2255	2280
C35RHA25	6	5.6	2235	2255
C35RHA30	6	5.2	2235	2255
C40RHA0	6	6.1	2260	2275
C40RHA15	6	5.2	2255	2280
C40RHA20	6	5.3	2245	2260

Table 7
Surface area of binder and volume fractions of aggregates, binder, paste, and mortar for different SCC mixtures

Concrete	Volume fraction of aggregates (m^3/m^3)	Volume fraction of binder (m^3/m^3)	Surface area of binder ($\times 10^3$ m^2/m^3)	Volume fraction of paste (m^3/m^3)	Volume fraction of mortar (m^3/m^3)
C30RHA0	0.635	0.156	202.78	0.156	0.365
C30RHA15	0.622	0.169	344.06	0.169	0.378
C30RHA20	0.615	0.172	388.92	0.172	0.385
C35RHA0	0.661	0.135	174.72	0.135	0.339
C35RHA5	0.655	0.138	214.70	0.138	0.345
C35RHA10	0.654	0.142	256.00	0.142	0.346
C35RHA15	0.650	0.145	296.15	0.145	0.351
C35RHA20	0.646	0.149	336.74	0.149	0.354
C35RHA25	0.637	0.151	374.48	0.151	0.363
C35RHA30	0.636	0.155	415.78	0.155	0.364
C40RHA0	0.673	0.117	151.76	0.117	0.328
C40RHA15	0.668	0.127	259.45	0.127	0.332
C40RHA20	0.664	0.130	294.52	0.130	0.336

effect is expected for orimet and inverted slump cone flow spreads. The increased paste volume and decreased aggregate content enhance the deformability of the concrete, as the frequency of contact and collision between coarse aggregates decreases during the deformation of fresh concrete [34]. However, the increased paste volume at lower W/B ratio and higher RHA content did not produce any significant influence on the slump of the concretes, as can be seen from Table 3. This is because the slump becomes less dependent on the paste volume in highly workable concretes such as SCC [35].

The W/B ratio and RHA content significantly influenced the orimet and inverted slump cone flow times of concrete (Table 3). The concrete flow time increased with lower W/B ratio and greater RHA content. This is because the volume fraction and surface area of binder were increased with lower W/B ratio and higher RHA content (Table 7). The greater volume fraction and surface area of binder make a concrete more viscous, and thus increase its flow time [36]. However, the aggregate content was reduced whereas the paste volume was increased with the lower W/B ratio and greater RHA content. The reduced aggregate content and the in- creased paste volume alleviate the viscous nature of concrete [28, 37]. However, the proportional increase in paste volume and reduction in aggregate content were not as substantial as the proportional increases in volume fraction and surface area of binder. Hence, the net effect enhanced the viscous nature of concrete, thus providing the higher flow time results during orimet and inverted slump cone flow tests.

4.6.2 Passing ability

The J-ring slump, slump cone–J-ring flow spread, orimet–J-ring flow spread, and inverted slump cone–J-ring flow spread were influenced by the W/B ratio and RHA content of the concretes. These passing ability properties increased with lower W/B ratio and greater RHA content, as evident from Table 4. This is due to increased paste volume and decreased aggregate content as discussed earlier in the case of the filling ability properties of the concretes with respect to slump, slump flow, and orimet and inverted slump cone flow spreads (Section 4.6.1). However, the effects of W/B ratio and RHA content on the J-ring slump were marginal, as obvious from Table 4. A similar trend was observed for the slump without J-ring.

4.6.3 Segregation resistance

The visual inspection was not effective to exhibit the effect of W/B ratio on the segregation resistance of concrete. This is because the concretes C30RHA0 (W/B: 0.30), C35RHA0 (W/B: 0.35) and C40RHA0 (W/B: 0.40) were equally good on the basis of visual observation, and no sign of segregation was noticed (Table 5 and Figs. 6–8). In contrast, the influence of RHA on the segregation resistance of concrete was evident. The visual inspection of the slump flow, orimet flow spread, and inverted slump cone flow spread revealed that the presence of RHA eliminated external bleeding from concrete. However, the increased RHA content caused mortar halo in slump flow, orimet flow spread, and inverted slump cone flow spread, thus indicating lower segregation resistance (Table 5 and Figs. 6–8). The appearance of mortar halo was due to a greater differential movement of mortar than coarse aggregates at the increased paste and mortar volumes with higher RHA content (Table 7).

4.6.4 Unit weight

The unit weight of the concretes without RHA was slightly reduced with higher W/B ratio (Table 6). The binder weight was lower at higher W/B ratio (Table 2). However, the aggregate weight increased at higher W/B ratio. But the percent increase in aggregate weight was much lower than the percent reduction in binder weight per unit volume of concrete. Therefore, the unit weight of concrete was decreased at higher W/B ratio. Also, the unit weight of most concretes decreased slightly with higher RHA content (Table 6). This is because RHA was lighter than cement. In addition, the fine and coarse aggregate contents decreased as the paste volume increased in the presence of RHA. However, the decrease in the unit weight of concrete caused by RHA was marginal (<3%). This is credited to the improved physical packing in fresh concrete due to the finer particle size of RHA as compared to cement.

4.6.5 Air content

The air content was prone to decrease with lower W/B ratio and higher RHA content. This is mostly due to the increased surface area of the binder caused by greater RHA and cement contents (Table 7). The increased surface area of the binder intensifies the viscous nature of concrete that tends to collapse some of the air-voids with increased internal pressure [38]. In addition, the increased cement and RHA contents required higher dosages of HRWR. The HRWR molecules impede the attachment of entrained air-voids onto the binding materials by reducing the attachment sites [38]. Thus, the air content of concrete are reduced with increased cement and RHA contents. Therefore, the demand for AEA increased progressively with lower W/B ratio and higher RHA content for the target air content in concrete (Table2).

4.7. Optimum RHA content

The optimum content of RHA was determined based on the consideration of several factors. It was found to depend on the W/B ratio of the concretes. The RHA content above 15% caused the concrete with 0.30 W/B ratio significantly viscous and thus the orimet flow time exceeded the maximum acceptable criterion for filling ability.

In contrast, the orimet flow time was within the acceptable range when 20% RHA was used in the concretes with 0.35 and 0.40 W/B ratios. However, the viscous nature of the concretes with 25% and 30% RHA contents at 0.35 W/B ratio remained considerably high and therefore the orimet flow time also exceeded the maximum acceptable criterion in these two cases. In addition, the RHA content greater than 15% required high dosages of HRWR to achieve the required filling ability and passing ability, particularly at lower W/B ratios. The HRWR dosages required in the cases of 20–30% RHA were significantly greater than the maximum dosage recommended by the manufacturer. An excessive HRWR dosage may cause concrete setting problem, thus delaying the hydration process. The demand for the AEA dosage for the target air content also became relatively high for the RHA content greater than 15%. Moreover, handling and mixing difficulties were experienced for the concretes including RHA content greater than 15%. Nevertheless, obtaining the required filling ability, passing ability and air content was not problematic in the presence of 15% RHA.

The RHA decreased the segregation resistance of concretes, as realized based on their VSI values. The maximum RHA content for the adequate segregation resistance depended on the W/B ratio of concrete. For example, the concrete C40RHA15 (W/B: 0.40) with 15% RHA provided good segregation resistance (VSI: 1), whereas the concrete C35RHA15 (W/B: 0.35) with 15% RHA exhibited low segregation resistance (VSI: 2). In addition, the adequate segregation resistance was obtained for the concretes C35RHA5 (W/B: 0.35) and C35RHA10 (W/B: 0.35), which were prepared with 5% and 10% RHA, respectively. Based on the results of visual inspection, 10–15% RHA content can be considered as the maximum suit- able content for segregation-resistant SCC. Also, this RHA content had no adverse effect on the unit weight of concrete. Hence, the overall test results suggest that 10–15% RHA can be selected as the optimum content for use in SCC.

5. Conclusions

The following conclusions are drawn based on the test results obtained from the present study:

a. The slump flow, inverted slump cone flow spread, and orimet flow spread without and with J-ring, that is, the filling ability and passing ability increased at lower W/B ratio and higher RHA content due to the decreased aggregate content and increased paste volume of concrete.

b. The filling ability and passing ability criteria were fulfilled for the SCC mixtures, except few concretes with a lower W/B ratio and RHA content greater than 15–20% that became highly viscous mostly due to increased volume fraction and excessive surface area of the binder.

c. The orimet and inverted slump cone flow times increased with lower W/B ratio and higher RHA content, thus indicating a reduction in the filling ability of concrete. This is greatly attributed to the increased volume fraction and surface area of the binder used in concrete.

d. No sign of segregation was observed for the concretes with-out RHA. However, the effect of W/B ratio on the segregation resistance of concrete was not evident during visual inspection. In contrast, the sign of segregation (mortar halo) was observed in the case of RHA concretes during visual observation although the bleeding was significantly reduced.

e. The unit weight of concrete slightly increased at lower W/B ratio due to greater binder content. Conversely, the unit weight marginally decreased with higher RHA content due to the lighter weight of RHA, and also as a result of the reduced fine and coarse aggregate contents at the increased paste volume of concrete.

f. The optimum RHA content was 10–15% based on the results of filling ability, passing ability, segregation resistance, unit weight, and air content. It was dependent of the W/B ratio used in concrete. An increased optimum content of RHA can be obtained when it is used in concrete with a higher W/B ratio.

REFERENCES

[1] Okamura H, Ouchi M. Self-compacting concrete-development, present and future. In: Skarendahl A, Petersson O, editors. Proceedings of the first international RILEM symposium on self-compacting concrete. Sweden: Stockholm; 1999. p. 3–14.

[2] Ozawa K, Mackawa K, Okamura H. High performance concrete based on the durability design of concrete structures. In: Proceedings of the second East Asia-Pacific conference on structural engineering and construction. Thailand: Chiang-Mai; 1989. p. 445–450.

[3] Khayat KH. Workability, testing, and performance of self-consolidating concrete. ACI Mater J 1999;96(3):346–53.

[4] Okamura H, Ozawa K. Mix design for self-compacting concrete. Concr Library of JSCE 1995;25:107–20.

[5] Okamura H, Ouchi M. Self-compacting concrete. Adv Concr Technol 2003;1(1):5–15.

[6] Persson B. A comparison between mechanical properties of self-compacting concrete and the corresponding properties of normal concrete. Cem Concr Res 2001;31(2):193–8.

[7] Zhu W, Bartos PJM. Permeation properties of self-compacting concrete. Cem Concr Res 2003;33(6):921–6.

[8] Lachemi M, Hossain KMA, Lambros V, Bouzoubaâ N. Development of costeffective self-consolidating concrete incorporating fly ash, slag cement, or viscosity-modifying admixtures. ACI Mater J 2003;100(5):419–25.

[9] Okamura H, Ozawa K. Self-compactable high-performance concrete in Japan. In: Zia P, editor. Proceedings of the international workshop on highperformance concrete. Thailand: Bangkok; 1994. p. 31–44.

[10] Mehta PK, Monteiro PJM. Concrete: Microstructure, properties, and materials, third ed. New York: USA: McGraw-Hill Companies, Inc.; 2006.

[11] Malhotra VM. Fly ash, slag, silica fume, and rice-husk ash in concrete: a review. Concr Int 1993;15(4):23–8.

[12] Zhang M-H, Malhotra VM. High-performance concrete incorporating rice husk ash as a supplementary cementing material. ACI Mater J 1996;93(6): 629–36.

[13] Memon SA, Shaikh MA, Akbar H. Utilization of rice husk ash as viscosity modifying agent in self-compacting concrete. Construct Build Mater 2011;25(2):1044–8.

[14] ASTM C 33. Standard specification for concrete aggregates. Annual book of ASTM standards, vol.04.02. Philadelphia, USA: American Society for Testing and Materials; 2004.

[15] ACI 211.4R-93. Guide for selecting proportions for high-strength concrete with portland cement and fly ash. ACI manual of concrete practice, part 1. Detroit, USA: American Concrete Institute; 2004.

[16] ASTM C 143/C 143M. Standard test method for slump of hydraulic-cement concrete. Annual book of ASTM standards, vol.04.02. Philadelphia, USA: American Society for Testing and Materials; 2004.

[17] Brameshuber W, Uebachs S. Practical experience with the application of selfcompacting concrete in Germany. In: Ozawa K, Ouchi M, editors. Proceedings of the second international symposium on self-compacting concrete. Japan: Tokyo; 2001. p. 687–95.

[18] Daczko JA. Stability of self-consolidating concrete, assumed or ensured? In: Shah SP, Daczko JA, Lingscheit JA, editors. Proceedings of the first North American conference on the design and use of self-consolidating concrete. USA: Chicago; 2002. p. 223–228.

[19] ASTM C 138/C 138M. Standard test method for density (unit weight), yield, and air content (gravimetric) of concrete. Annual book of ASTM standards, vol.04.02. Philadelphia, USA: American Society for Testing and Materials; 2004.

[20] ASTM C 231. Standard test method for air content of freshly mixed concrete by pressure method. Annual book of ASTM standards, vol.04.02. Philadelphia, USA: American Society for Testing and Materials; 2004.

[21] Hu C, de Larrard F. The rheology of fresh high-performance concrete. Cem Concr Res 1996;26(2):283–94.

[22] Yen T, Tang C-W, Chang C-S, Chen K-H. Flow behaviour of high strength high performance concrete. Cem Concr Compos 1999;21(5–6):413–24.

[23] Aïtcin P-C. The use of superplasticizers in high performance concrete. In: Malier Y, editor. High performance concrete: from material to structure. London, UK: E & FN Spon; 1994. p. 14–33.

[24] EFNARC. Specifications and guidelines for self-consolidating concrete. Surrey, UK: European Federation of Suppliers of Specialist Construction Chemicals (EFNARC); 2002.

[25] SCCEPG. The European guidelines for self-compacting concrete: specification, production and use. West Midlands, UK: Self-compacting Concrete European Project Group (SCCEPG), The European Federation of Concrete Admixtures Associations; 2005.

[26] ACI 201.2R-01. Guide to durable concrete. ACI manual of concrete practice, part 1. Detroit, USA: American Concrete Institute; 2004.

[27] Bonen D, Shah SP. Fresh and hardened properties of self-consolidating concrete. Prog Struct Eng Mater 2005;7(1):14–26.

[28] Okamura H, Ozawa K, Ouchi M. Self-compacting concrete. Struct Concr 2000;1(1):3–17.

[29] Khayat KH, Assaad J. Air void stability in self-consolidating concrete. ACI Mater J 2002;99(4):408–16.